

METHODOLOGY

Open Access



# High throughput procedure utilising chlorophyll fluorescence imaging to phenotype dynamic photosynthesis and photoprotection in leaves under controlled gaseous conditions

Lorna McAusland<sup>1\*</sup> , Jonathan A. Atkinson<sup>1</sup>, Tracy Lawson<sup>2</sup> and Erik H. Murchie<sup>1</sup>

## Abstract

**Background:** As yields of major crops such as wheat (*T. aestivum*) have begun to plateau in recent years, there is growing pressure to efficiently phenotype large populations for traits associated with genetic advancement in yield. Photosynthesis encompasses a range of steady state and dynamic traits that are key targets for raising Radiation Use Efficiency (RUE), biomass production and grain yield in crops. Traditional methodologies to assess the full range of responses of photosynthesis, such as leaf gas exchange, are slow and limited to one leaf (or part of a leaf) per instrument. Due to constraints imposed by time, equipment and plant size, photosynthetic data is often collected at one or two phenological stages and in response to limited environmental conditions.

**Results:** Here we describe a high throughput procedure utilising chlorophyll fluorescence imaging to phenotype dynamic photosynthesis and photoprotection in excised leaves under controlled gaseous conditions. When measured throughout the day, no significant differences ( $P > 0.081$ ) were observed between the responses of excised and intact leaves. Using excised leaves, the response of three cultivars of *T. aestivum* to a user-defined dynamic lighting regime was examined. Cultivar specific differences were observed for maximum PSII efficiency ( $F_v'/F_m' - P < 0.01$ ) and PSII operating efficiency ( $F_q'/F_m' - P = 0.04$ ) under both low and high light. In addition, the rate of induction and relaxation of non-photochemical quenching (NPQ) was also cultivar specific. A specialised imaging chamber was designed and built in-house to maintain gaseous conditions around excised leaf sections. The purpose of this is to manipulate electron sinks such as photorespiration. The stability of carbon dioxide ( $\text{CO}_2$ ) and oxygen ( $\text{O}_2$ ) was monitored inside the chambers and found to be within  $\pm 4.5\%$  and  $\pm 1\%$  of the mean respectively. To test the chamber, *T. aestivum* 'Pavon76' leaf sections were measured under at 20 and 200  $\text{mmol mol}^{-1}$   $\text{O}_2$  and ambient  $[\text{CO}_2]$  during a light response curve. The  $F_v'/F_m'$  was significantly higher ( $P < 0.05$ ) under low  $[\text{O}_2]$  for the majority of light intensities while values of NPQ and the proportion of open PSII reaction centers (qP) were significantly lower under  $> 130 \mu\text{mol m}^{-2} \text{s}^{-1}$  photosynthetic photon flux density (PPFD).

**Conclusions:** Here we demonstrate the development of a high-throughput ( $> 500$  samples  $\text{day}^{-1}$ ) method for phenotyping photosynthetic and photo-protective parameters in a dynamic light environment. The technique exploits chlorophyll fluorescence imaging in a specifically designed chamber, enabling controlled gaseous environment around leaf sections. In addition, we have demonstrated that leaf sections do not differ from intact plant material even  $> 3$  h after sampling, thus enabling transportation of material of interest from the field to this laboratory based

\*Correspondence: lorna.mcausland@nottingham.ac.uk

<sup>1</sup> Division of Plant and Crop Science, School of Biosciences, University of Nottingham, Sutton Bonington Campus, Sutton Bonington, Leicestershire LE12 5RD, UK

Full list of author information is available at the end of the article



platform. The methodologies described here allow rapid, custom screening of field material for variation in photosynthetic processes.

**Keywords:** Photosynthesis, Photo-protection, Chlorophyll fluorescence, Dynamic, Phenotyping, Imaging, Wheat

## Background

Plant phenotyping or phenomics is defined as the high throughput quantification of relevant plant and crop traits for research or breeding purposes and includes growth, morphology, photosynthesis and biochemistry, often exploiting the most recent advances in image analysis [1]. While the area of genomic profiling and DNA sequencing have advanced rapidly in recent years, phenotyping methods are still entering into common research practice to complement large-scale crop improvement and still developing in terms of throughput and resolution [2–5]. Consequently, phenotyping is still considered a bottle-neck for advancing biomass and yield in crop species where such techniques can be used to identify novel breeding traits but currently take considerable time to collect and analyse [2, 6, 7]. With the added complexity of environmental plasticity and plethora of phenotypic parameters to choose from, plant phenomics benefits from large interdisciplinary collaborations where methodologies can be rapidly disseminated. The ultimate aim is the integrated assessment of key phenotypic traits in combination with application of genomic data of large plant populations—a prerequisite for linkage mapping or genome-wide association mapping of quantitative trait loci; correlating sections of DNA with quantitative phenomic attributes [8–12].

Improving photosynthesis in major crop species is a key phenotypic trait associated with higher biomass production, grain yield and Radiation Use Efficiency (RUE—biomass produced per unit radiation intercepted). Currently, it is estimated that C3 crops convert between 1 and 2% of solar energy to biomass of a possible 4.5%. CO<sub>2</sub> enrichment studies (FACE) [13, 14] and Zhu et al. [15] have demonstrated that modern crop species have the capacity to improve photosynthetic efficiency by 2–3.5% [16]. However, photosynthesis is not a single trait, but rather the product of a series of linked processes including biochemical capacity (e.g. carboxylation and electron transport), anatomical characteristics (e.g. stomatal and mesophyll conductance) and the ability of the plant to interact with dynamic environmental conditions [17]. Each of these processes can be assessed using techniques such as gas exchange, spectroscopy and microscopy but these tend to be low throughput, slow and labour intensive and often only assessed at a single time point. Phenotyping cereal crops presents additional problems including the size of the plant, its 3-dimensional

complexity and the need to capture the correct developmental stage [18, 19]. For example, the size of a wheat plant and the complex array of leaves in space with multiple occlusions creates problems for applying chlorophyll fluorescence imaging technology where leaves should be illuminated evenly, the distance of plant to sensor needs to be known with some precision and a period of dark adaptation of leaves may be required. With high numbers of lines required for genetic mapping or crossing programs, traditional physiological techniques often fall short of providing the large volumes of data required for accurate predictions required to improve molecular breeding strategies.

Chlorophyll fluorescence (CF) is a rapid and non-invasive, high resolution technique to determine changes in photochemistry through monitoring the fluorescence emission of photosystem II (PSII) in situ [20–24]. For example, at 2% oxygen, photorespiration is virtually eliminated; therefore, the products of linear electron transport can be directly related to those used in CO<sub>2</sub> assimilation. Under these conditions, the PSII operating efficiency ( $F_q'/F_m'$ ) is positively and directly correlated with the rate of CO<sub>2</sub> assimilation [23, 25, 26]. Measurements of chlorophyll fluorescence are non-invasive and can be used in imaging setups [21, 27], in combination with other techniques [28] and even remotely on a large scale [29]. Devices can be cheap and simple [30], or highly complex and linked to gas exchange to measure processes such as photorespiration under low oxygen [20].

Imaging leaves or whole plants using chlorophyll fluorescence provides data on the spatial and temporal response of PSII to fluctuating environmental conditions such as Photosynthetic Photon Flux Density (PPFD), CO<sub>2</sub> and O<sub>2</sub>. In the field, plants are continuously responding to changing environmental conditions and it is increasingly apparent that assessment of *dynamic* responses is key to the identification of lines that either maintain or improve yields in the field [17]. Recent studies have emphatically shown the importance of the dynamic photosynthetic responses to crop yield and plant productivity both with gas exchange measurements [31, 32] and chlorophyll fluorescence [33], leading to identification of lines of interest. For example, chlorophyll fluorescence has been used to: determine carbon assimilation rate under low [O<sub>2</sub>] [27]; to analyse transgenic lines for improved photo-protective de-activation kinetics and improved crop biomass

[33] and finally, to assessing plants in which the photorespiratory pathway has been manipulated leading to improved yield [34, 35].

Here, we describe a novel method for screening photosynthetic efficiency in wheat leaves and show for the first time the feasibility of using excised leaf tissue as a highly convenient means to achieve accurate, rapid quantification of complex dynamic shifts in photosynthetic efficiency and photoprotection in a high throughput fashion. Importantly this overcomes some of the practical limitations of phenotyping large numbers of field grown cereal plants. We present designs for a custom-adapted imaging chamber to applying user-defined gas concentrations within the measurement system. The methodology described here facilitates the screening of 100+ individual mature plants simultaneously (several hundred plants day<sup>-1</sup>) in response to complex, custom dynamic light protocols for temporal assessment of PSII processes.

## Methods

### Overview of the screening pipeline

An overview of the screening pipeline using a large population of wheat plants is shown in Fig. 1. At a set developmental stage (e.g. flag leaf emergence—growth

stage 41–42 according to the Decimal Code System [36]), approximately 2 cm<sup>2</sup> leaf material is excised and placed on damp paper towel. For transportation, these samples are positioned between two sheets of glass and placed in an insulated box to prevent large temperature changes. Sampling of 100 plants takes between 15 and 20 min. The plates are then transported to a customised FluorCam CF imager (FC800-222, Photon systems instruments, Drasov, Czech Republic) and arranged inside the custom chamber (see ‘Imaging Chamber Design’ for details of customisation). During a standard screen the leaf sections are dark adapted for 1 h. This rapid sampling procedure allows numerous leaf sections from glasshouse or field grown plants to be imaged simultaneously. The PPFD protocol can either be manufacturer or user defined. Using the custom imaging chambers (see ‘Imaging Chamber Design’), leaf sections can also be screened under controlled gaseous conditions (See ‘Timing and Control of Gases’). Typically, the gases are turned on 45 min into the hour and the pressure and concentrations of CO<sub>2</sub> and O<sub>2</sub> are monitored using sensors (Qubit Systems Inc., Kingston, Canada). On the hour (and after conditions are constant within the chamber) the selected protocol is run.

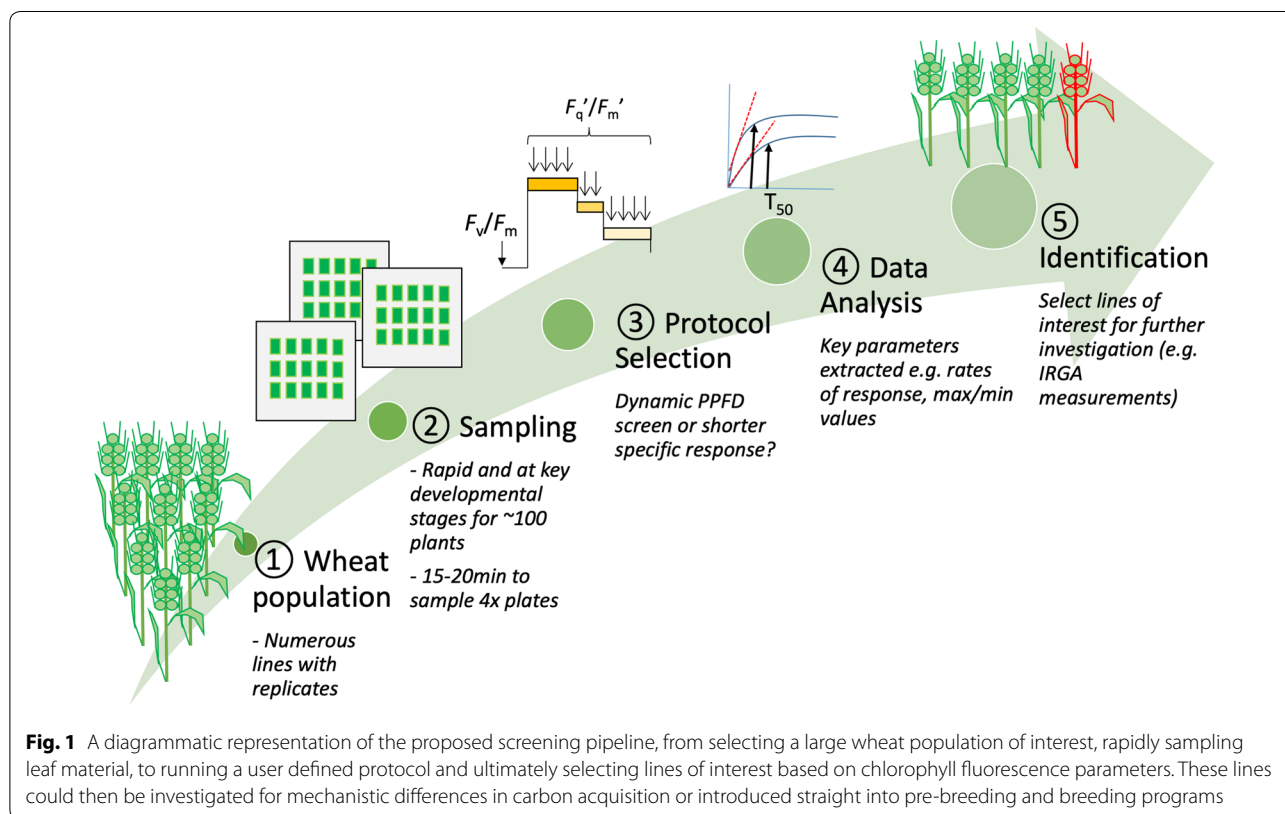


**Fig. 1** A diagrammatic representation of the proposed screening pipeline, from selecting a large wheat population of interest, rapidly sampling leaf material, to running a user defined protocol and ultimately selecting lines of interest based on chlorophyll fluorescence parameters. These lines could then be investigated for mechanistic differences in carbon acquisition or introduced straight into pre-breeding and breeding programs

### Technical properties of the chlorophyll fluorescence imager

Chlorophyll fluorescence imaging was performed using a customised FluorCam imaging fluorometer fitted with a white and red LED panel (Additional file 1: Fig. S1). Shutter time and sensitivity of the charge-coupled device (CCD) were adjusted in accordance with sample. The FluorCam is located in a temperature controlled dark room maintained between 20 and 22 °C.

Modern fluorometers commonly use a modulated light source at a known frequency to induce chlorophyll fluorescence—otherwise known as pulse-amplitude modulated (PAM) fluorescence—where the detector is set to measure at the same frequency as the excitation [37]. This methodology allows measurements to occur when the plant is illuminated. During a typical measurement, the plant is dark adapted (between 20 and 60 min) to allow maximal plastoquinone A ( $Q_A$ ) oxidation after which the leaf is exposed to a saturating flash of light that maximally reduces  $Q_A$ , closing all PSII reaction centres. This procedure gives a maximum fluorescence value ( $F_m$ ) and, in the light, allows the separation of the photochemical (e.g. PSII operating efficiency— $F_q'/F_m'$ ) and non-photochemical (e.g. Non-photochemical quenching—NPQ) processes in the leaf under specific photosynthetic photon flux density (PPFD) conditions. The parameter  $F_q'/F_m'$ , also termed  $\Phi$ PSII or quantum yield (QY), is a measure of the proportion of absorbed light utilised by PSII and therefore can also be used, in combination with measurements of leaf absorbance, to calculate linear electron transport rate (ETR). These parameters (Table 1) are key in the identification of differences between different

lines, treatments (biotic or abiotic) or genotypes [20–22, 38, 39]. Many instruments are available for assessment of these parameters either as spot measurements or as images. The benefit of imaging chlorophyll fluorescence is the ability to analyse both temporal and spatial variation in PSII efficiency [28].

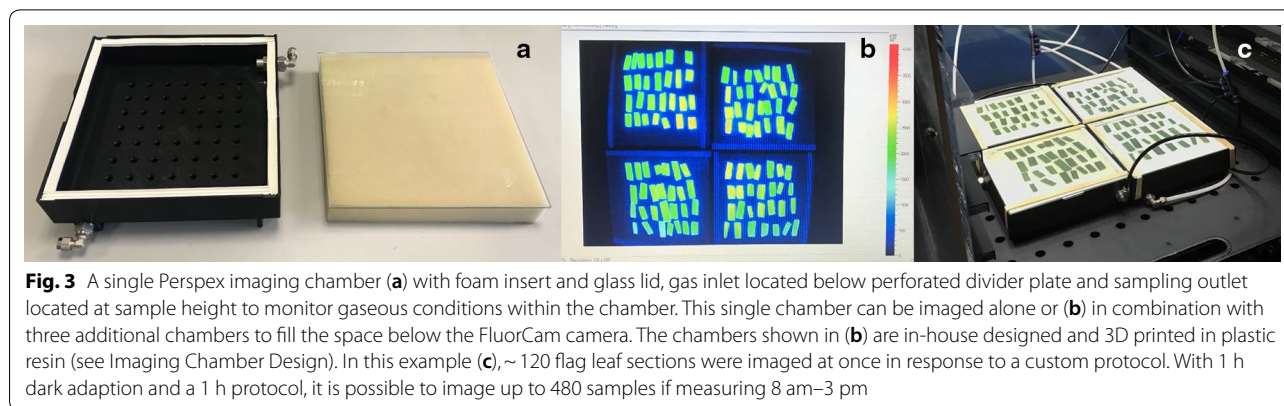
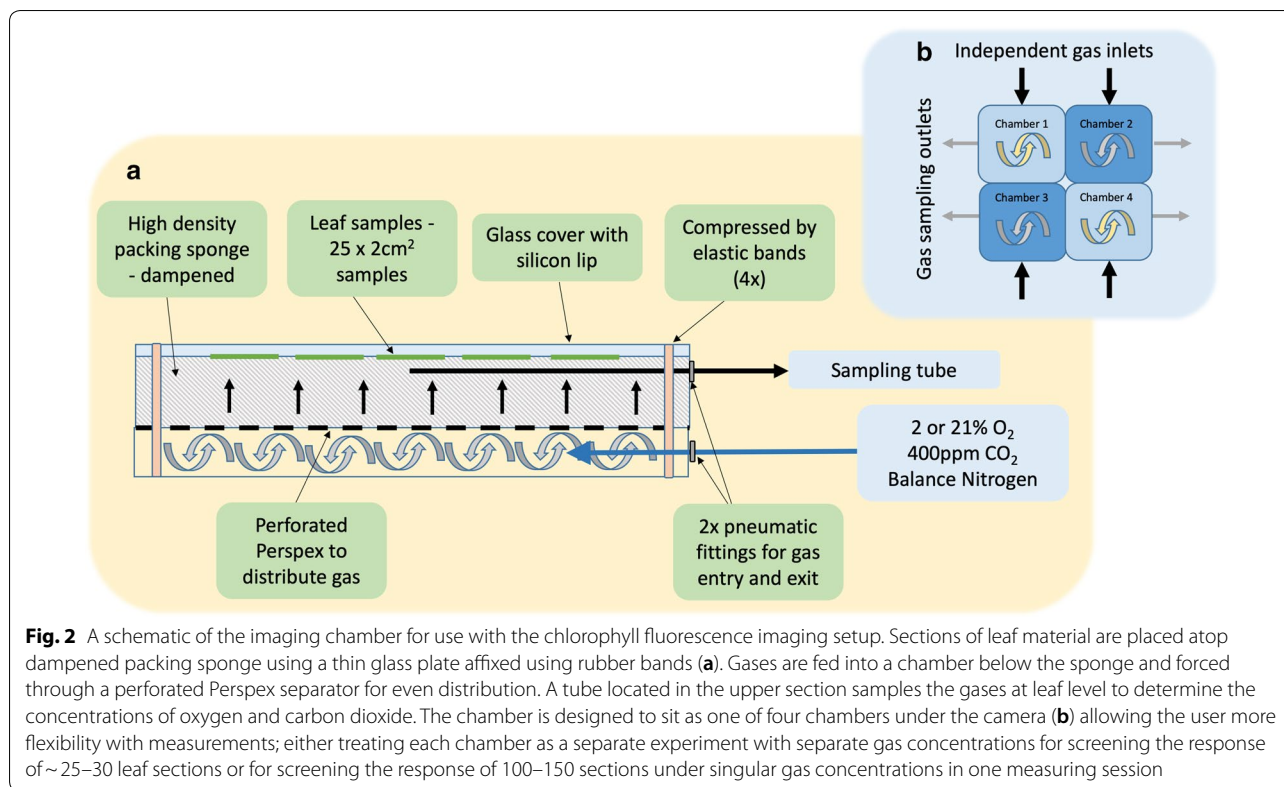
### Custom imaging chamber for controlling measuring environment

In order to control concentrations of  $O_2$  and  $CO_2$  around the leaf sections, four chambers were designed and constructed in-house (Figs. 2 and 3). The chambers measure 20 cm (length)  $\times$  20 cm (width)  $\times$  10 cm (depth). A separate, perforated divider halves the chamber (Fig. 3a), forcing gas flow over an even area and through a high-density sponge soaked in water (2.8 mm thick). This sponge sits on the divider and humidifies the dry, cylinder-supplied air. A rubber seal on the top edge of the chamber provides a better gas seal to stabilise gaseous conditions in the chamber. Leaf sections are positioned, adaxial side-up, on the dampened sponge and a glass plate laid on top to produce a flat surface to image. Rubber bands provide further compression around each side of the chamber and further stabilise the concentration of gases at leaf level. Gas enters through 6  $\times$  4 mm (OD  $\times$  ID) PTFE tubing via a 6 mm (OD) pneumatic fitting located in the lower half of the chamber. To monitor gas concentrations at leaf level, a second 6 mm fitting is located in the top half the chamber at the furthest point from gas entry. The chambers allow imaging of approximately 25–30 mature *T. aestivum* flag leaf sections (2 cm  $\times$  3 cm) per chamber—in total 100–120 samples per measurement

**Table 1 Commonly used abbreviations and equations employed when measuring chlorophyll fluorescence**

Parameter	Formula	Definition
$F, F', F'_s$	n/a	Steady state fluorescence emission from dark- or light-adapted (') leaf, respectively. $F'$ is sometimes referred to as $F'_s$ when at steady state.
$F_m, F'_m$	n/a	Maximal chlorophyll fluorescence measured in a dark- or light-adapted state respectively
$F_o, F'_o$	n/a	Minimal chlorophyll fluorescence measured in a dark- or light-adapted state respectively
$F_v, F'_v$	n/a	Variable chlorophyll fluorescence measured as the difference between dark- or light-adapted $F_m/F_m'$ and $F_o/F_o'$ .
$F_v/F_m$	$(F_m - F_o)/F_m$	Maximum quantum efficiency of PSII.
$F'_v/F'_m$	$(F'_m - F'_o)/F'_m$	Maximum efficiency of PSII in the light.
$F_q'/F'_m$	$(F'_m - F')/F'_m$	PSII operating efficiency: the quantum efficiency of PSII electron transport in the light. AKA $\Phi$ PSII, quantum yield or $\Delta F/F'_m$
ETR or $J$	$\Phi$ PSII (AKA $F_q'/F'_m$ ) $\times$ PPFDa $\times$ (0.5)	Linear electron transport rate; where PPFDa is absorbed light ( $\mu\text{mol m}^{-2} \text{s}^{-1}$ ) and 0.5 is a factor that accounts for the partitioning of energy between PSII and PSI.
NPQ	$(F_m - F'_m)/F'_m$	Non-photochemical quenching: estimates the rate constant for heat loss from PSII.
qL	$(F_q'/F'_v)/(F'_o'/F')$	Estimates the fraction of open PSII centers ( $Q_A$ oxidized); considered a more accurate indicator of the PSII redox state than qP
qP	$(F'_m - F')/(F'_m - F'_o)$ AKA $F_q'/F'_v$	Photochemical quenching: relates PSII maximum efficiency to operating efficiency. Non-linearly related to proportion of PSII centers that are open. 1–qP has also been used to denote proportion of closed centers

A summary table of the commonly used chlorophyll fluorescence parameters and corresponding equations. For a more comprehensive review please refer to Murchie and Lawson [21], Baker [20] and Maxwell and Johnson [22]



session is all four chambers (Fig. 3b) are used (Fig. 3c). Separate gas cylinders (British Oxygen Company, UK) supply either synthetic pressurised air (approximately containing 400  $\mu\text{mol mol}^{-1}$   $\text{CO}_2$  and 210  $\text{mmol mol}^{-1}$   $\text{O}_2$ ) or a pre mixed 20  $\text{mmol mol}^{-1}$  oxygen, 400  $\mu\text{mol mol}^{-1}$   $\text{CO}_2$  in nitrogen. As an alternative to the synthetic or pre-mixed gases, mass flow controllers with cheaper industrial standard gases could be used instead. Gas flow was manipulated manually to maintain stable gaseous conditions within the chambers. Chamber  $\text{CO}_2$ ,  $\text{O}_2$  and pressure were monitored using the calibrated sensors (S102 and S151, Qubit Systems, Kingston, Canada). Flow to the

sensors was determined using a rotameter to maintain flows at 500  $\text{ml min}^{-1}$ . Data was logged using Logger Pro. (Vernier, Coalville, UK) and the sampling time adjusted depending on experiment; typically measurements were taken every 15 s throughout a protocol.

The chambers were designed using Fusion 360 (Autodesk, San Rafael, CA, USA) and 3D printed using an Ultimaker S5 printer in Ultimaker Tough PLA (Ultimaker, Geldermalsen, Neatherlands). Four separate chambers were printed and are designed to be used as separate chambers (i.e. filling with different gas concentrations simultaneously) or as a single unit (i.e. all chambers filling

with the same gas concentration). This flexibility allows application of a highly controllable screen for the response of photosynthetic traits to complex environmental fluctuations at same time but also provides a high throughput screen when phenotyping large populations of plants.

The CAD files for the final chamber design are fully available with this manuscript (Additional file 2) including printer settings and additional notes, so that users can either print their own, outsource the printing or modify the designs. The design could also be constructed using Perspex sheets if access to a 3D printer is not available (written instructions and necessary tools not listed).

### Plant material and cultivation

The modern wheat cultivars *T. aestivum* 'Paragon', 'Pavon76' and 'Highbury', the landrace *T. aestivum* 'CS94' were grown (April–October 2017) in a glasshouse at Sutton Bonington, Leicestershire, UK. Glasshouse conditions were maintained at 22–18 °C ± 2 °C (day/night) under regular mildew, aphid, and thrips control measures applied following the manufacturers' recommendations. Plants received supplemental lighting (Son-T, Philips, Surrey, UK) to 16 h light or when PPFD fell below 500  $\mu\text{mol m}^{-2} \text{s}^{-1}$ . For comparing live leaf samples to excised leaf samples, 3 week old seedlings grown in compost (Levington F2S, Scotts, Bramford, UK) filled 12 well trays. To analyse larger leaf sections plants were grown individually in 2L pots, automatically irrigated twice daily for approximately 1 min with feed (HortiMix Standard, Hortifeeds, Lincoln, UK).

### Description of measurements

The white LED light was used as the actinic source for all protocols described in this paper (Additional file 1: Fig. S1). All samples were dark adapted inside the chamber for 1 h before a saturating pulse (5500  $\mu\text{mol m}^{-2} \text{s}^{-1}$  PPFD, duration 800 ms) was taken to measure  $F_v/F_m$ . Any increases in PPFD occurred immediately after this measurement.

In order to assess any physiological differences between the responses of whole leaves and excised leaf sections, 3 week old seedlings of *T. aestivum* 'Paragon' and leaf sections of the same age were measured simultaneously using the FluorCam and a single imaging chamber. Leaf sections were excised in the glasshouse, immediately placed between dampened tissues and placed in an insulated box for transportation to the lab. In the lab, the sections were aligned on damp sponge while live material was carefully tucked under the glass top plate of the chamber. To determine the length of time that leaf samples could be measured after excision without a negative impact on PSII, light response curves were conducted every hour for 9am to 5 pm allowing a 1 h dark adaption period between

measurements. The light curve protocol consists of six subsequent saturating pulses taken every 60 s at the end of a step-wise increases from 26 to 1140  $\mu\text{mol m}^{-2} \text{s}^{-1}$  PPFD. Prior to every light response curve, a measurement of  $F_v/F_m$  was taken.

To determine variation between modern wheat bread wheat cultivars, *T. aestivum* cv.'Paragon', 'Pavon76' and the landrace *T. aestivum* 'Chinese Spring 94' were grown. Flag leaf sections (GS40-41) were excised at 9 am and allowed to dark-adapt for 1 h in the imaging chamber. Fifteen minutes before the initial saturating pulse to determine  $F_v/F_m$  was taken, ambient air was used to saturate the chamber to ensure consistent  $\text{CO}_2$  and  $\text{O}_2$  concentrations around the samples. The protocol consisted of three consecutive light-steps of 15 min; 500  $\mu\text{mol m}^{-2} \text{s}^{-1}$ , 100  $\mu\text{mol m}^{-2} \text{s}^{-1}$  and 1000  $\mu\text{mol m}^{-2} \text{s}^{-1}$  PPFD. Saturating pulses were taken every minute throughout the protocol.

To determine the stability and ease of switching between different gas concentrations in the chambers, four chambers were connected to a compressed synthetic air gas supply (British Oxygen Company, UK), and sealed using the glass lids and bands (Figs. 3 and 4). The gases were turned on and  $\text{O}_2$ ,  $\text{CO}_2$  and atmospheric pressure were monitored every 15 s. After 10 min, the synthetic gas supply was switched to a commercial premix 2%  $\text{O}_2$  (20 mmol  $\text{mol}^{-1}$   $\text{O}_2$ , 385  $\mu\text{mol mol}^{-1}$   $\text{CO}_2$  and  $\text{N}_2$  balance—British Oxygen Company, UK). After three 10 min switches, a 15 min period of each of the gases was demonstrated.

Finally, to ascertain the impact of low oxygen on chlorophyll fluorescence parameters, flag leaf sections were harvested from *T. aestivum* 'Pavon76' at 9am and exposed to either compressed synthetic air (180 mmol  $\text{mol}^{-1}$   $\text{O}_2$  and 380  $\mu\text{mol mol}^{-1}$   $\text{CO}_2$ ,  $\text{N}_2$  balance) or 2% oxygen (20 mmol  $\text{mol}^{-1}$   $\text{O}_2$ , 385  $\mu\text{mol mol}^{-1}$   $\text{CO}_2$  and  $\text{N}_2$  balance). Forty-five minutes into the dark adaption the gases were turned on, flooding the chamber. Gaseous conditions inside the chamber were allowed to stabilise for 15 min.  $F_v/F_m$  was measured, followed by a light response curve. The values of  $F_v/F_m$  and the responses of  $F_v'/F_m'$ ,  $F_q'/F_m'$ , qP and NPQ were extracted from each protocol.

### Determining the rates of relaxation and induction in NPQ

In order to determine the rate of NPQ relaxation (Eq. 1) and induction (Eq. 2) data was fitted using a 2-factor exponential decline to minimum (Eq. 1) or rise to maximum (Eq. 2) using curve fitting toolbox in Matlab (Matlab R2018a, USA).

$$y = a \cdot e(-b \cdot x) \quad (1)$$

$$y = a \cdot e^{-bx} \quad (2)$$

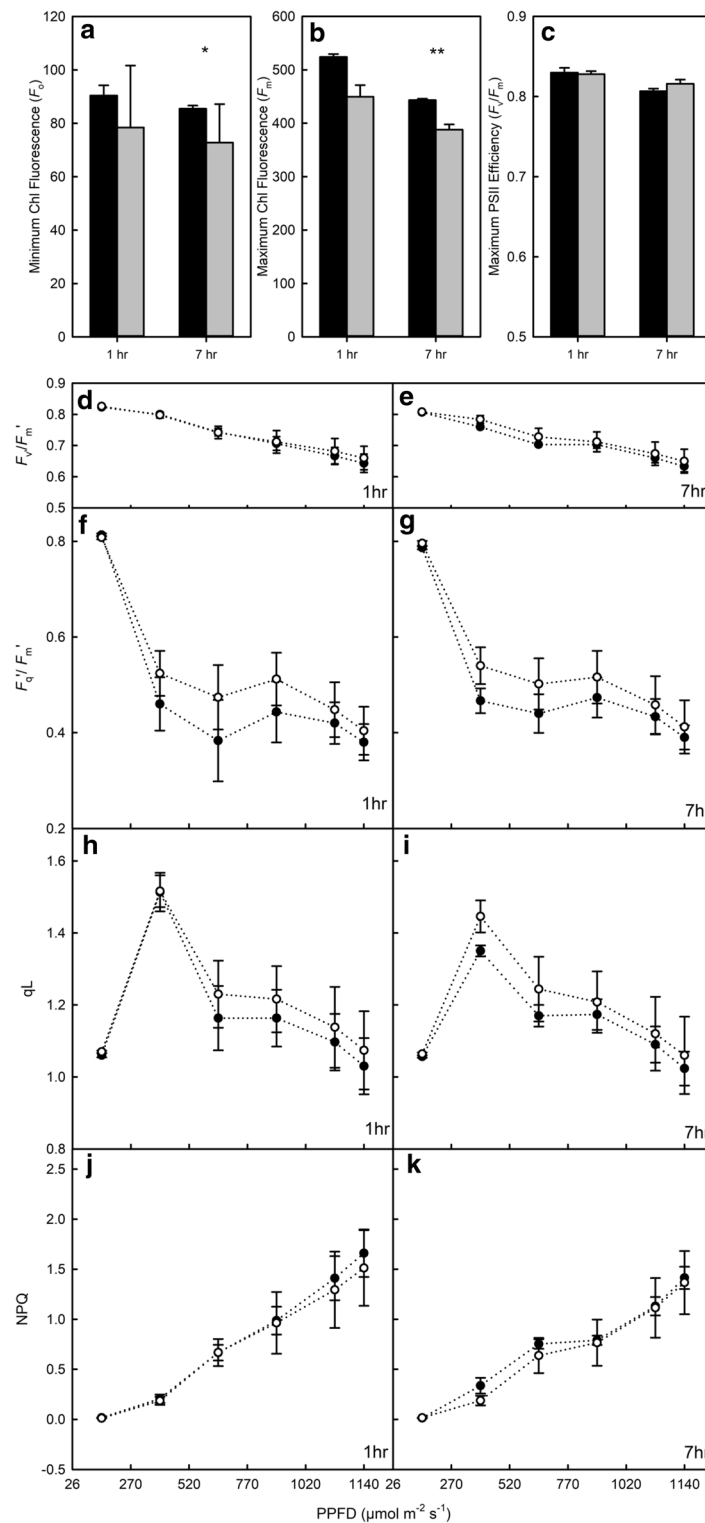


**Fig. 4** Minimum (a— $F_0$ ) and maximum (b— $F_m$ ) fluorescence signal after 1 and 7 h in the imaging chamber for intact leaf material (black) and excised (grey) leaf tissue. From these values, the maximum PSII efficiency (c— $F_v/F_m$ ) was calculated. Subsequent measurements of maximum PSII efficiency in the light ( $F_v'/F_m'$ , d and e), PSII operating efficiency ( $F_q'/F_m'$ , f and g), the fraction of open PSII centres (qL—h and i) and non-photochemical quenching (NPQ—j and k) were calculated in response to increasing light intensity for excised (white circle) and intact (black circle) leaf material (n = 3–5) for 1 and 7 h after sampling. See Table 1 for full descriptions of chlorophyll fluorescence parameters. Asterisks indicate significant differences between excised and intact tissue, where \*\*\*\* $P < 0.001$  \*\*\* $P < 0.01$  \*\* $P < 0.05$

where  $a$  is the initial value and  $b$  a constant representing the rate of exponential decay or growth. In order to determine the time ( $t$ ) taken to achieve either 50% of the maximum NPQ values ( $I_{50}$ ) or 50% of the minimum NPQ values ( $R_{50}$ ) the equations were solved for  $b$  and the following calculations applied;

$$t = 1/b$$

$$t * \ln(2)$$

where  $t$  is the time constant and  $b$  is the rate obtained from the rearrangement of either Eq. 1 or Eq. 2.

### Statistical analyses

Statistical analyses were conducted in R (<http://www.r-project.org/>). A Shapiro–Wilk test was used to test for normality and a Levene’s test of homogeneity was used to determine if samples had equal variance. Single factor differences were analysed using a one-way ANOVA with a Tukey–Kramer honest significant difference (HSD) test where more than one group existed or using a Student’s  $t$  test where only two groups were compared.

## Results

### Comparing the diurnal response of intact leaf material with leaf sections

In order to assess physiological differences between the responses of whole leaves and excised leaf sections, seedlings of *T. aestivum* ‘Paragon’ and leaf sections of the same age were measured simultaneously using the FluorCam (Fig. 4) over a 7 h time period. After the first dark adaption period, the intact material demonstrated no significant difference in  $F_o$  and  $F_m$  respectively compared to the excised material (Fig. 4a, b). However, it is important to note that the trend in these constituents of  $F_v/F_m$  was consistent throughout the day regardless of treatment (Fig. 4c). After 7 h in the chamber, values of  $F_m$  and  $F_o$  were significantly ( $P < 0.05$ ) higher in the intact leaf tissue, however this did not lead to a significant difference in  $F_v$ . Similarly, when comparing  $F_v/F_m$  values 1 h and 7 h after sampling, there was no difference in values between the intact or excised leaves ( $P = 0.79$ ). Immediately after measuring  $F_v/F_m$ , a light response curve was taken. During the curve, a general decrease in maximum PSII efficiency in the light ( $F_v'/F_m'$ —Fig. 4d, e), PSII operating efficiency ( $F_q'/F_m'$ —Fig. 4f, g) and the fraction of open PSII centres (qL—Fig. 4h, i) was observed for the leaf treatments. Non-photochemical quenching (NPQ—Fig. 4j, k) increased with increasing PPFD. But with no significant differences observed over time for any of the response parameters measured during the light response curve ( $P > 0.2$ ). No significant differences were determined between the responses measured 1 h or 7 h after

sampling when comparing just the intact leaves or the excised leaf tissue ( $P > 0.081$ ).

### Identifying variation in the response of PSII for cultivars of *T. aestivum*

To identify variation in the magnitude of change and kinetic response of PSII, leaf sections from *T. aestivum* ‘Paragon W07/08’, ‘Pavon76’ and ‘CS94’ were subjected to step changes in PPFD after an initial measurement of  $F_v/F_m$  (Fig. 5). No significant differences ( $F_{(2,9)} = 0.36$ ,  $P = 0.705$ ) were observed between the cultivars  $F_v/F_m$ , with all leaf sections achieving  $0.81 \pm 0.01$ . When illuminated with 500 and 1000  $\mu\text{mol m}^{-2} \text{s}^{-1}$  PPFD, ‘Pavon76’ achieved significantly higher ( $P < 0.03$ ) values of  $F_m$  when compared to the other modern cultivar ‘Paragon W07/08’ (data not shown). Following the measurement of  $F_v/F_m$ , the leaf sections were exposed to 500 (15 min), 100 (10 min) and 1000 (10 min)  $\mu\text{mol m}^{-2} \text{s}^{-1}$  PPFD. Maximum PSII efficiency in the light ( $F_v'/F_m'$ , Fig. 5a), PSII operating efficiency ( $F_q'/F_m'$ —Fig. 5b) and non-photochemical quenching (NPQ—Fig. 5c) reached steady-state in 5–10 min under 500  $\mu\text{mol m}^{-2} \text{s}^{-1}$  PPFD while the fraction of open PSII centres (qL—Fig. 5d) never achieved steady state. In general, the response to subsequent light-steps of 100 and 1000  $\mu\text{mol m}^{-2} \text{s}^{-1}$  PPFD was more rapid.

During the light-step treatment, ‘Paragon W07/08’ demonstrated the lowest  $F_v'/F_m'$  values under both 500 and 1000  $\mu\text{mol m}^{-2} \text{s}^{-1}$  PPFD (Fig. 5a), significantly lower than those measured in ‘Pavon76’ and ‘CS94’ ( $F_{(2,9)} = 17.86$ ,  $P < 0.013$ ). Conversely, ‘Paragon W07/08’ demonstrated the highest values of NPQ (Fig. 5c), significantly higher than those measured for ‘Pavon76’ and ‘CS94’ under 500 and 1000  $\mu\text{mol m}^{-2} \text{s}^{-1}$  PPFD ( $F_{(2,9)} = 16.68$ ,  $P < 0.001$  and  $F_{(2,9)} = 26.9$ ,  $P < 0.0002$  respectively). No significant differences were observed between plants under the two high light steps for  $F_q'/F_m'$  (Fig. 5b), however ‘CS94’ achieved significantly higher values ( $P < 0.04$ ) under 100  $\mu\text{mol m}^{-2} \text{s}^{-1}$  PPFD when compared to the modern cultivars ‘Paragon W07/08’ and ‘Pavon76’.

In order to determine differences in the rate of NPQ relaxation ( $R_{50}$ —500 to 100  $\mu\text{mol m}^{-2} \text{s}^{-1}$  PPFD) and induction ( $I_{50}$ —100 to 1000  $\mu\text{mol m}^{-2} \text{s}^{-1}$  PPFD), single factor exponential functions were fitted to sections of the response data (see “Statistical analyses”). In general, all three cultivars showed a slower relaxation of NPQ on transfer to low light compared to the time taken to fully induce NPQ under high light (Table 2) which is generally consistent with the known kinetics of NPQ and its regulation by PsbS and the xanthophyll cycle [33]. Although no significant differences were noted for either  $I_{50}$  or  $R_{50}$  between cultivars, a general

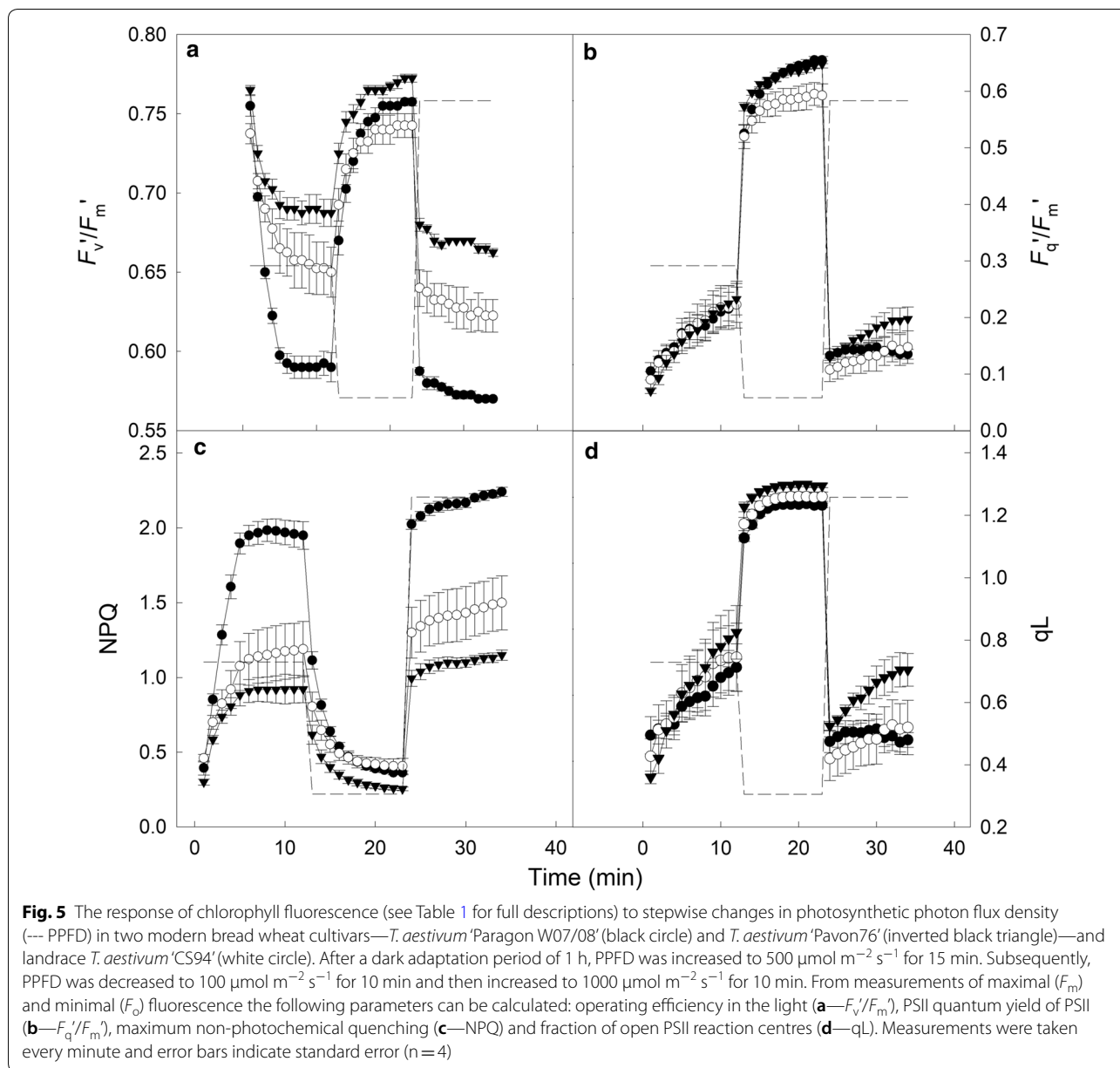


**Fig. 5** The response of chlorophyll fluorescence (see Table 1 for full descriptions) to stepwise changes in photosynthetic photon flux density (--- PPFD) in two modern bread wheat cultivars—*T. aestivum* 'Paragon W07/08' (black circle) and *T. aestivum* 'Pavon76' (inverted black triangle)—and landrace *T. aestivum* 'CS94' (white circle). After a dark adaptation period of 1 h, PPFD was increased to 500  $\mu\text{mol m}^{-2} \text{s}^{-1}$  for 15 min. Subsequently, PPFD was decreased to 100  $\mu\text{mol m}^{-2} \text{s}^{-1}$  for 10 min and then increased to 1000  $\mu\text{mol m}^{-2} \text{s}^{-1}$  for 10 min. From measurements of maximal ( $F_m$ ) and minimal ( $F_0$ ) fluorescence the following parameters can be calculated: operating efficiency in the light (a— $F_v'/F_m'$ ), PSII quantum yield of PSII (b— $F_q'/F_m'$ ), maximum non-photochemical quenching (c—NPQ) and fraction of open PSII reaction centres (d— $qL$ ). Measurements were taken every minute and error bars indicate standard error ( $n=4$ )

**Table 2** Response of non-photochemical quenching to step-decreases (relaxation) and increases (induction) in PPFD

Cultivar	Relaxation 500 to 100 $\mu\text{mol m}^{-2} \text{s}^{-1}$ PPFD			Induction 100 to 1000 $\mu\text{mol m}^{-2} \text{s}^{-1}$ PPFD		
	Min. NPQ	$R_{50}$ (s)	Decrease in NPQ (%)	Max. NPQ	$I_{50}$ (s)	Fold increase
Paragon W07/08	0.37 ± 0.018	124.5 ± 6.6	81.3 ± 0.7*	2.2 ± 0.0*	5 ± 1.4	6.2 ± 0.3*
CS94	0.43 ± 0.058	108.6 ± 5.8	64.8 ± 3.2	1.5 ± 0.3	4.1 ± 1.3	3.7 ± 0.5
Pavon76	0.26 ± 0.012	67.9 ± 1.0	71.9 ± 1.8	1.2 ± 0.0	9 ± 1.5	4.5 ± 0.2

Example parameters extracted from the response of non-photochemical quenching (NPQ) in leaf sections of *T. aestivum* 'Paragon W07/08', 'CS94' and 'Pavon76' shown in Fig. 5. Measurements were taken every minute under step-wise changes in Photosynthetic Photon Flux Density (PPFD) from 500 (15 min), 100 (10 min) to 1000  $\mu\text{mol m}^{-2} \text{s}^{-1}$  (10 min). The minimum and maximum NPQ values were determined under 100 and 1000  $\mu\text{mol m}^{-2} \text{s}^{-1}$  PPFD respectively. In addition, the percentage decrease (500 to 100  $\mu\text{mol m}^{-2} \text{s}^{-1}$  PPFD) and fold-increase (100–1000  $\mu\text{mol m}^{-2} \text{s}^{-1}$ ) in NPQ were calculated. Lastly, a 2-factor exponential decay function was used to determine the time taken to achieve half the minimum (relaxation— $R_{50}$ ) or maximum (induction— $I_{50}$ ) NPQ (see 'Determining the rates of relaxation and induction in NPQ'). Data are the mean ± SE ( $n=3-4$ ). Asterisks indicate significant differences where \*\*\*\* $P < 0.001$  \*\*\* $P < 0.01$  \*\* $P < 0.05$

trend was observed that cultivars with higher NPQ values under high PPFD took longer to relax when light intensity was decreased. Modern cultivar ‘Paragon W07/08’ showed the highest values in NPQ under  $1000 \mu\text{mol m}^{-2} \text{s}^{-1}$  PPFD ( $P < 0.04$ ), took the longest to relax under  $100 \mu\text{mol m}^{-2} \text{s}^{-1}$  PPFD and demonstrated the greatest percentage decline in magnitude (Table 2). Conversely, the lowest values of NPQ under 100 and  $1000 \mu\text{mol m}^{-2} \text{s}^{-1}$  PPFD were observed for ‘Pavon76’, which relaxed in the shortest amount of time but took over 3 s longer to achieve half the maximum NPQ under  $1000 \mu\text{mol m}^{-2} \text{s}^{-1}$  PPFD when compared to ‘Paragon W07/08’ or ‘CS94’.

#### Timing and control of gases inside the imaging chamber

At  $20 \text{ mmol m}^{-2} \text{O}_2$ , photorespiration is inhibited and the fluorescence parameter  $F_q'/F_m'$  is linearly related to the rate of photosynthetic  $\text{CO}_2$  uptake [23, 25]. Therefore, it was essential that that  $[\text{O}_2]$  within the chamber was (a) stable and (b) able to be manipulated to rapidly switch between atmospheric  $[\text{O}_2]$  to  $20 \text{ mmol m}^{-2}$ . As an example, during the measurement of typical light response curve, the chosen  $[\text{O}_2]$  would have to be maintained for approximately 15 min while CF images are being taken.

In the example shown in Fig. 6, low  $[\text{O}_2]$  was achieved in  $< 120 \text{ s}$  and was maintained within 1% of the target value for several minutes before returning to

near-ambient conditions within 135 s. After three 10 min switches, a 15 min period of both low  $[\text{O}_2]$  and ambient  $[\text{O}_2]$  are demonstrated. Figure 6 also illustrates the stability of  $[\text{CO}_2]$  ( $376 \mu\text{mol mol}^{-1} \pm 4.5\%$ ) within the chamber.

#### Screening leaf sections under ambient and low oxygen

Under  $20 \text{ mmol mol}^{-1} \text{O}_2$ , photorespiration is inhibited and  $\text{CO}_2$  assimilation represents the major sink for the end-products of electron transport (ATP and NADPH) [20, 40]. Leaf sections of *T. aestivum* cv. ‘Pavon76’ were imaged under low and ambient  $\text{O}_2$  concentrations (see Fig. 7). The maximum quantum efficiency of PSII photochemistry ( $F_v/F_m$ —Fig. 7a), maximum quantum efficiency of PSII photochemistry in the light ( $F_v'/F_m'$ —Fig. 7b),  $F_q'/F_m'$  (Fig. 7c), photochemical quenching (qP—Fig. 7d) and NPQ (Fig. 7e) were measured in response to stepwise increases in PPFD from 0 to  $1140 \mu\text{mol m}^{-2} \text{s}^{-1}$ . These responses were first measured under  $20 \text{ mmol mol}^{-1} \text{O}_2$  followed by  $200 \mu\text{mol mol}^{-1} \text{O}_2$ . No significant difference ( $P = 0.15$ ) was observed between  $F_v/F_m$  values under low or ambient  $\text{O}_2$  (Fig. 7a). Similarly, during the protocol, no significant differences were noted for  $F_m'$  ( $P > 0.061$ ) or  $F_o'$  ( $P > 0.31$ ). In general, values of  $F_v'/F_m'$  were higher under low oxygen, with measurements taken under  $520 \mu\text{mol m}^{-2} \text{s}^{-1}$  being significantly higher ( $P < 0.05$ ) than the values obtained under ambient oxygen concentrations.

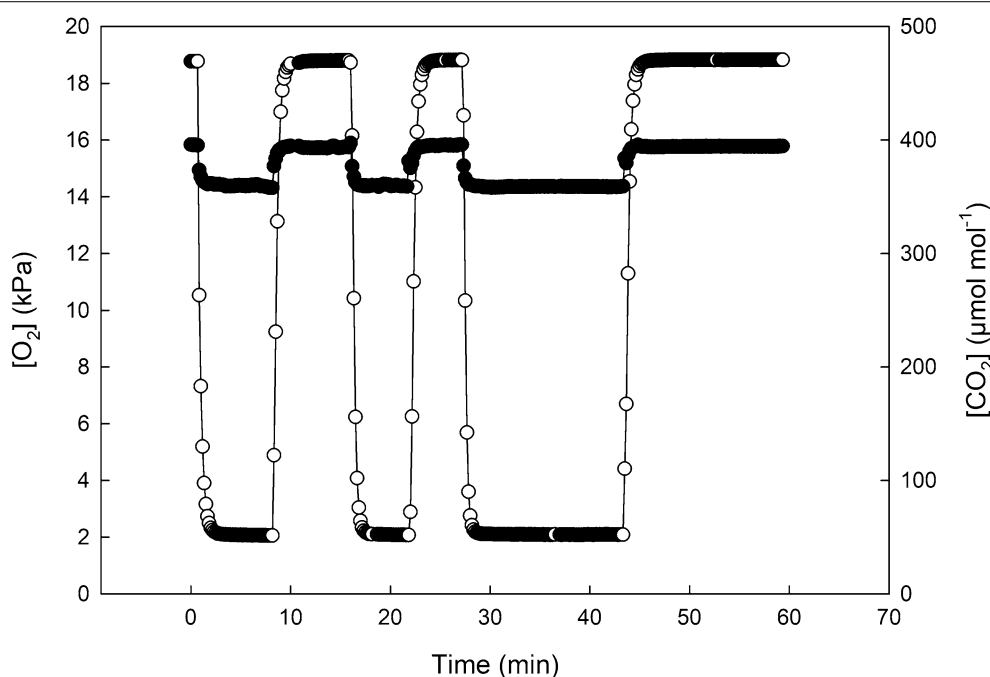


**Fig. 6** Concentrations of  $\text{O}_2$  (white circle) and  $\text{CO}_2$  (black circle) in the measuring chamber during an experiment. Measurements were taken every 15 s. Oxygen concentration was switched from ambient compressed air (19 kPa) to 2 kPa three times while maintaining  $375 \pm 18 \mu\text{mol mol}^{-1} \text{CO}_2$

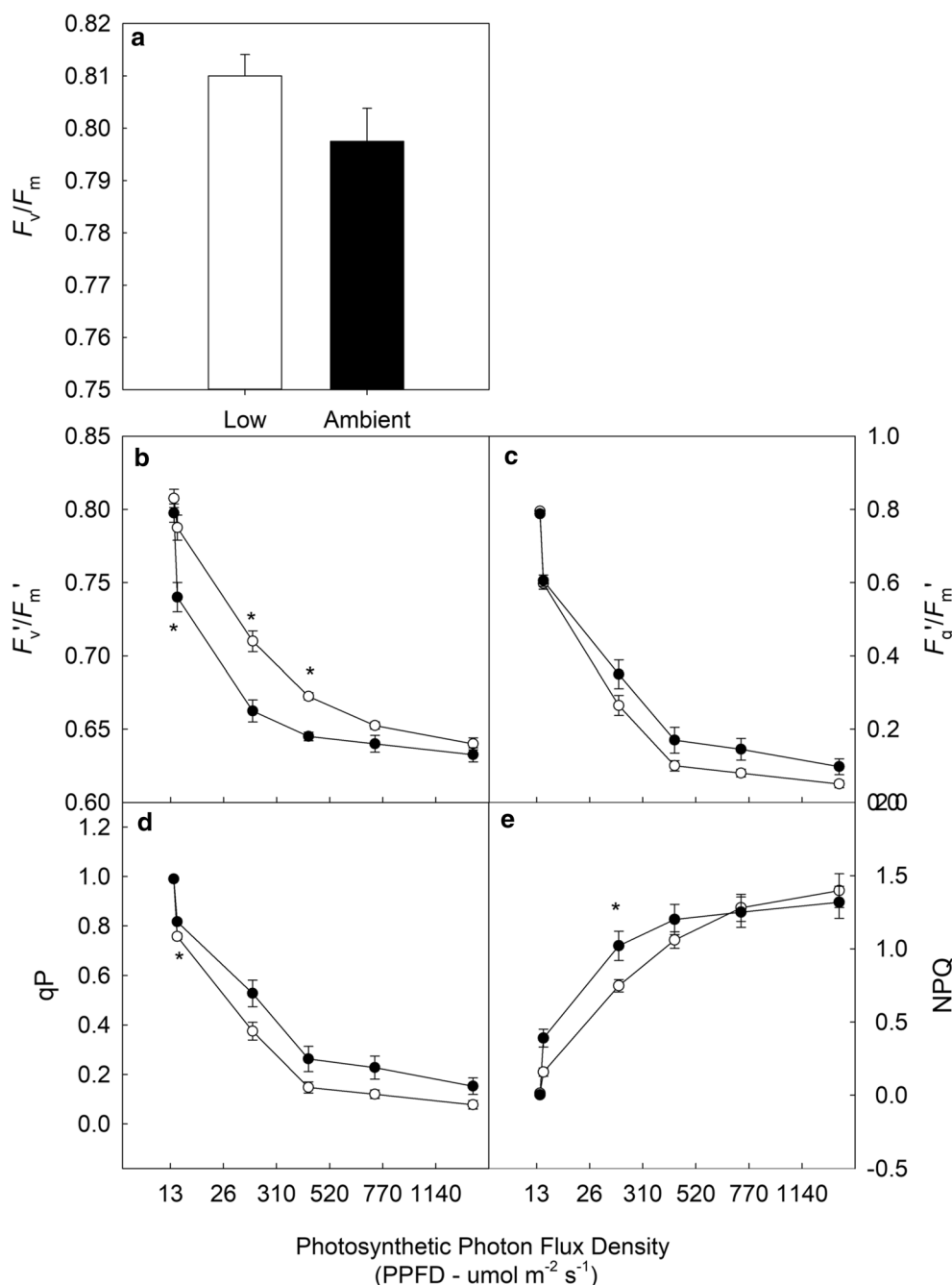


**Fig. 7** The response of chlorophyll fluorescence parameters (see Table 1 for full descriptions) in the wheat cultivar *T. aestivum* 'Pavon76' to stepwise increases in Photosynthetic Photon Flux Density (PPFD) from 0 to 100% (0–1027  $\mu\text{mol m}^{-2} \text{s}^{-1}$  PPFD) under 20 (white circle) or 200 (black circle)  $\text{mmol mol}^{-1} \text{O}_2$ . After a dark adaptation period of 1 h, maximum PSII efficiency was determined (a— $F_v/F_m$ ). From the dark-adapted values of maximal ( $F_m$ ) and minimal ( $F_o$ ) fluorescence, the following parameters can be calculated: operating efficiency in the light (b— $F_v'/F_m'$ ), PSII quantum yield of PSII (c— $F_q'/F_m'$ ), fraction of open PSII reaction centres (d—qP) and non-photochemical quenching (e—NPQ) and. Data are the mean  $\pm$  SE (n = 4). Asterisks indicate significant differences where \*\*\*\* $P < 0.0001$  \*\*\* $P < 0.001$  \*\* $P < 0.01$  \* $P < 0.05$

In general, values of  $F_q'/F_m'$ , qP and NPQ were lower under low oxygen conditions but these differences were only significant at low light intensities for NPQ and qP.

**Discussion**

This study describes the amalgamation of high throughput PAM-based chlorophyll fluorescence imaging with

rapid sampling and screening of wheat (*T. aestivum*) leaf sections under controlled gaseous environments. This methodology provides the means to rapidly phenotype high numbers of plants for changes in the state of PSII under controlled environmental conditions and in response to user-determined PPFD perturbations. The work presented in this paper demonstrates that excised leaf tissue is representative of intact material for such photosynthetic assays (Fig. 4) and has potential to contribute to technologies to alleviate the bottleneck in phenotyping large populations of glasshouse or field grown plants.

#### Excised wheat leaf material is representative of intact material

Numerous physiological measurements still employ leaf sections as a means to determining variation between plants [41–43], and while invasive, the imaging of leaf sections increases the number of individuals measured at one developmental stage and at one time point. The user is less limited by the size of the CF imager and more by the number of plants that can be grown at the facility—making this system a cost effective, high throughput option for phenotyping plant populations.

As shown in Fig. 4, the response of excised leaf tissue was representative of the intact leaf material, both in response to PPFD and over the 9 h measurement period. This has important implications in logistics of screening large populations—allowing researchers to sample, transport and measure material in the timeframe of a day without the worry of sample degradation. Maintaining on damp tissue at the temperature of sampling (~20–24 °C) seems to be the optimal method of transporting the lamps to the CF imager, while cooling samples (<10 °C) may have negative implications for photosynthesis [44, 45] and leaf metabolite composition [46] over time. We suggest that a further development of this technique is a simplified design that is suitable for moving to a field location. This would require an appropriate power supply.

#### Flexible screening technologies improve selection power

The development of custom, semi-gas tight chambers to arrange the samples increases the capability of the system, providing the means to screen under non-photorespiratory conditions or to supply a custom gas mix e.g. anaerobic conditions or saturating CO<sub>2</sub>. Assessment of photosynthetic processes under different gas mixtures adds extra strength to the screen. For example, at low (20 mmol mol<sup>-1</sup>) oxygen, the relative contribution of photorespiration can be estimated and a linear

relationship between  $F_q'/F_m'$  and the quantum yield of CO<sub>2</sub> assimilation (and therefore linear electron flux) can be accurately monitored between samples [20, 25, 28]. When imaged at low oxygen, the excised leaf sections had higher values of  $F_v'/F_m'$ , which were significantly higher at the majority of light intensities, but lower values of  $F_q'/F_m'$  and qP (Fig. 7). This data suggests that under low oxygen, the leaf sections exhibited greater maximum PSII efficiency that was not realised in the other CF parameters for this cultivar. This implies variation in the capacity of PSII to assimilate CO<sub>2</sub>, a trait which can be further investigated using traditional techniques (such as IRGAs) to determine, for example, Rubisco kinetics.

Coupling this technology with other imaging technologies to increase the overall predictive power of the system e.g. screening for absorbance, reflectance indices, and stomatal density. For example, it has been shown that glaucousness can decrease light absorbance in barley leaves by up to 12% [47], therefore limiting light acquisition and decreasing leaf temperature under the lower light levels experienced in the canopy [48]. Accounting for this developmental disparity in a large population of high leaf index species (such as wheat), perhaps using scoring or reflectance indices and coupling with the method of chlorophyll fluorescence screening discussed here, would increase a breeder or researchers selection power. In this example, the rapid, systematic screening of a selection of leaf-level traits has the potential to aid the identification of lines able to maintain or increase yields under fluctuating environmental conditions experienced in the field. The ability to monitor photosynthetic processes under fluctuating PPFD conditions also provides a powerful tool in determining complex, often hierarchical, photosynthetic responses.

The temporal response of photosynthesis to fluctuating light has gathered growing interest in recent years as the technology for producing rapidly adjustable PPFD environments and PSII monitoring is more accessible to researchers [49]. Plants are subject to changes in spectral quality and intensity of PPFD during the growing season; constantly adapting and acclimating to optimise the conversion of CO<sub>2</sub> to biomass and, ultimately, yield [49–51]. Whether the photosynthetic acclimation to the PPFD environment is a dynamic (reversible) or developmental (morphological), diversity in light acclimation exists between different species [52] and the methodology described here can provide rapid identification of dynamic differences between large populations of monocropped plants, determining individuals which will optimally respond to the light environments and improve identification of potentially high yielding varieties.

For example, the response of NPQ has been previously identified as a target for improvement [53], with the rate of relaxation thought to inhibit CO<sub>2</sub> fixation between 5.5 and 30% in tobacco [33]. These observations indicated that there is an optimum value in the magnitude and rate of NPQ induction and relaxation for crop species. While rapid up-regulation of NPQ (e.g. over expression of PSII protein, PsbS [41]) may serve to protect a plant during high light or rapidly fluctuating conditions, a slow relaxation or downregulation may inhibit CO<sub>2</sub> assimilation. The timing of induction and relaxation presented in this paper demonstrated a significant degree of variability in the time taken to induce and relax NPQ (Table 2) however, it was noted a line which achieved faster inductions under high light did not necessarily achieve a faster relaxation under low light. The term NPQ encompasses mechanisms employed by the photosynthetic machinery to regulate the thermal dissipation of excess excitation energy [20]. These processes are mainly associated with activity of the xanthophyll cycle [54, 55], PsbS and protonation of PSII antennae proteins [56]. The data presented in this paper suggests there is variation to be exploited for improvement, especially as pre-breeding and breeding programs are now generating cultivars with wild relative or land race genomic introgressions as a means to improve genetic diversity in our modern varieties [57, 58]. Phenotyping using the screening method discussed in this paper has a two-fold role; the identification of variation within the generated population and linking that variation to a wild or landrace parent.

Extrapolating both steady-state and the timing of chlorophyll fluorescence parameter responses (e.g. NPQ) highlight a rapid and simple method of screening high numbers of plants for differences in the magnitude and rate of response of PSII to PPFD. From this data, efforts can be concentrated on larger populations of smaller numbers of lines for the greatest differences in photosynthesis. Here we provide one example: the Watkins core collection is a set of genetically diverse landraces consisting of 119 accessions. Using the method outlined in this paper it would take between 1 and 2 days to perform a simple PPFD-based screen on a population of 476 plants (assuming four replicates). To increase the efficiency of this process a seedling screen could be performed prior to vernalisation (therefore cutting down on valuable glasshouse and growth room space), and then again at physiologically relevant growth stages; flag leaf, booting, anthesis and post anthesis. There is no other technique to our knowledge that is capable of such throughput and resolution in terms of dynamic photosynthesis and photoprotection.

## Conclusions

The methodology described here demonstrates a rapid, novel high throughput approach for phenotyping photosynthetic processes in a major crop species under controlled PPFD and gaseous conditions. We have demonstrated that excised tissues can be used as a robust proxy for intact leaf material and, with this method, exposed cultivar-specific responses to dynamic PPFD protocols. Furthermore, we have built and tested custom imaging chambers, capable of maintaining gaseous concentrations around excised leaves during protocols to provide the user control over this additional environmental variable. This overcomes logistical and practical problems of rapidly applying such sophisticated dynamic light protocols during CF analyses on large plants such as cereals. Finally, we have discussed the logistics of screening > 500 samples per day using this methodology to contribute a wealth of phenotypic data and improve selection power in large populations of wheat with the ultimate aim of improving yield through improved photosynthesis and RUE.

## Supplementary information

**Supplementary information** accompanies this paper at <https://doi.org/10.1186/s13007-019-0485-x>.

**Additional file 1: Figure S1.** The spectrum of the white (-) and measuring (...) light sources used with the FluorCam. The 'white' light source peaks at 448 and 553 nm while the measuring light peaks at 617 nm. Spectra shown were measured as the average of 10 spectrums.

**Additional file 2.** Supplementary information and files on the design and construction of the custom imaging chambers.

## Acknowledgements

This work was funded by the Biotechnology and Biological Sciences Research Council [BB/N021061/1]. This work was performed as part of the International Wheat Yield Partnership (Project number IWYP48). We thank The Nottingham BBSRC Wheat Research Centre team for providing seeds of the *T. aestivum* cultivars and Dr D. Wells for useful discussions on the design, construction and implementation of the imaging chambers. TL acknowledges the support of the Biotechnology and Biological Sciences Research Council through BB/N021061/1. We would like to thank the Future Food Beacon and School of Biosciences, University of Nottingham for financial support provided to LM during the writing of this manuscript.

## Authors' contributions

LM, EM and TL devised the initial concept of a high throughput gas-specific dynamic screen; LM led the further development and refinement of the hardware and software; LM developed the methodology, conducted experiments and analysed results. LM and JAA designed the imaging chamber while JAA constructed and printed the prototypes and final chamber. LM, EM and TL combined to interpret the results. LM and EM wrote the manuscript with contributions from TL and JAA. All authors read and approved the final manuscript.

## Funding

This work was funded by the Biotechnology and Biological Research Council [Grant Number BB/N021061/1] and the University of Nottingham Future Food Beacon of Excellence. This work formed part of the International Wheat Yield Partnership project 'Wider, Faster: high-throughput phenotypic exploration of novel genetic variation for breeding high biomass and yield in wheat' (IWYP48).

**Availability of data and materials**

The datasets analysed during the current study are available from the corresponding author on reasonable request.

**Ethics approval and consent to participate**

Not applicable.

**Consent for publication**

Not applicable.

**Competing interests**

The authors declare that they have no competing interests.

**Author details**

<sup>1</sup> Division of Plant and Crop Science, School of Biosciences, University of Nottingham, Sutton Bonington Campus, Sutton Bonington, Leicestershire LE12 5RD, UK. <sup>2</sup> School of Life Sciences, University of Essex, Wivenhoe Park, Colchester, Essex CO4 3SQ, UK.

Received: 24 May 2019 Accepted: 14 August 2019

Published online: 18 September 2019

**References**

- Araus JL, Kefauver SC, Zaman-Allah M, Olsen MS, Cairns JE. Translating high-throughput phenotyping into genetic gain. *Trends Plant Sci.* 2018;23(5):451–66.
- Araus JL, Cairns JE. Field high-throughput phenotyping: the new crop breeding frontier. *Trends Plant Sci.* 2014;19(1):52–61.
- Fahlgren N, Gehan MA, Baxter I. Lights, camera, action: high-throughput plant phenotyping is ready for a close-up. *Curr Opin Plant Biol.* 2015;24:93–9.
- Li L, Zhang Q, Huang D. A review of imaging techniques for plant phenotyping. *Sensors.* 2014;14(11):20078–111.
- Mishra KB, Mishra A, Klem K. Plant phenotyping: a perspective. *Indian J Plant Physiol.* 2016;21(4):514–27.
- Ghanem ME, Marrou H, Sinclair TR. Physiological phenotyping of plants for crop improvement. *Trends Plant Sci.* 2015;20(3):139–44.
- Tardieu F, Cabrera-Bosquet L, Pridmore T, Bennett M. Plant phenomics, from sensors to knowledge. *Curr Biol.* 2017;27(15):770–83.
- Atwell S, Huang YS, Vilhjálmsson BJ, Willems G, Horton M, Li Y, Meng D, Platt A, Tarone AM, Hu TT. Genome-wide association study of 107 phenotypes in *Arabidopsis thaliana* inbred lines. *Nature.* 2010;465(7298):627.
- Flood PJ, Harbinson J, Aarts MG. Natural genetic variation in plant photosynthesis. *Trends Plant Sci.* 2011;16(6):327–35.
- Huang X, Sang T, Zhao Q, Feng Q, Zhao Y, Li C, Zhu C, Lu T, Zhang Z, Li M. Genome-wide association studies of 14 agronomic traits in rice landraces. *Nat Genet.* 2010;42(11):961.
- Yang W, Guo Z, Huang C, Duan L, Chen G, Jiang N, Fang W, Feng H, Xie W, Lian X. Combining high-throughput phenotyping and genome-wide association studies to reveal natural genetic variation in rice. *Nat Commun.* 2014;5:5087.
- van Bezouw RF, Keurentjes JJ, Harbinson J, Aarts MG. Converging phenomics and genomics to study natural variation in plant photosynthetic efficiency. *Plant J.* 2019;97(1):112–33.
- Long SP, Marshall-Colon A, Zhu X-G. Meeting the global food demand of the future by engineering crop photosynthesis and yield potential. *Cell.* 2015;161(1):56–66.
- Long SP, Ainsworth EA, Leakey AD, Nösberger J, Ort DR. Food for thought: lower-than-expected crop yield stimulation with rising CO<sub>2</sub> concentrations. *Science.* 2006;312(5782):1918–21.
- Zhu X-G, Long SP, Ort DR. What is the maximum efficiency with which photosynthesis can convert solar energy into biomass? *Curr Opin Biotechnol.* 2008;19(2):153–9.
- Long SP, ZHU XG, Naidu SL, Ort DR: can improvement in photosynthesis increase crop yields? *Plant Cell Environ.* 2006;29(3):315–30.
- Murchie EH, Kefauver S, Araus JL, Muller O, Rascher U, Flood PJ, Lawson T. Measuring the dynamic photosynthome. *Ann Bot.* 2018;122(2):207–20.
- Carmo-Silva E, Andralojc PJ, Scales JC, Driever SM, Mead A, Lawson T, Raines CA, Parry MA. Phenotyping of field-grown wheat in the UK highlights contribution of light response of photosynthesis and flag leaf longevity to grain yield. *J Exp Bot.* 2017;68(13):3473–86.
- Driever S, Lawson T, Andralojc P, Raines C, Parry M. Natural variation in photosynthetic capacity, growth, and yield in 64 field-grown wheat genotypes. *J Exp Bot.* 2014;65(17):4959–73.
- Baker NR. Chlorophyll fluorescence: a probe of photosynthesis *in vivo*. *Annu Rev Plant Biol.* 2008;59:89–113.
- Murchie E, Lawson T. Chlorophyll fluorescence analysis: a guide to good practice and understanding some new applications. *J Exp Bot.* 2013;64(13):3983–98.
- Maxwell K, Johnson GN. Chlorophyll fluorescence—a practical guide. *J Exp Bot.* 2000;51(345):659–68.
- Genty B, Briantais JM, Baker NR. The relationship between the quantum yield of photosynthetic electron transport and quenching of chlorophyll fluorescence. *Biochim Biophys Acta Gen Subj.* 1989;990(1):87–92.
- Genty B, Meyer S. Quantitative mapping of leaf photosynthesis using chlorophyll fluorescence imaging. *Funct Plant Biol.* 1995;22(2):277–84.
- Genty B, Harbinson J, Baker N. Relative quantum efficiencies of the two photosystems of leaves in photorespiratory and non-photorespiratory conditions. *Plant Physiol Biochem.* 1990;28(1):1–10.
- Cornic G. Drought stress and high light effects on leaf photosynthesis. In: Baker NR, Bowyer JR, editors. *Photoinhibition of photosynthesis*. Oxford: BIOS Scientific Publishers Ltd.; 1994. p. 297–313.
- Barbagallo RP, Oxborough K, Pallett KE, Baker NR. Rapid, non invasive screening for perturbations of metabolism and plant growth using chlorophyll fluorescence imaging. *Plant Physiol.* 2003;132(2):485–93.
- McAusland L, Davey P, Kanwal N, Baker N, Lawson T. A novel system for spatial and temporal imaging of intrinsic plant water use efficiency. *J Exp Bot.* 2013;64(16):4993–5007.
- Meroni M, Rossini M, Guanter L, Alonso L, Rascher U, Colombo R, Moreno J. Remote sensing of solar-induced chlorophyll fluorescence: review of methods and applications. *Remote Sens Environ.* 2009;113(10):2037–51.
- Kuhlger S, Austic G, Zegarac R, Osei-Bonsu I, Hoh D, Chilvers MI, Roth MG, Bi K, TerAvest D, Weebadde P. MultispeQ Beta: a tool for large-scale plant phenotyping connected to the open PhotosynQ network. *R Soc Open Sci.* 2016;3(10):160592.
- Matthews JS, Viallet-Chabrand SR, Lawson T. Acclimation to fluctuating light impacts the rapidity and diurnal rhythm of stomatal conductance. *Plant Physiol.* 2018;176(3):1939–51.
- McAusland L, Viallet-Chabrand S, Matthews J, Lawson T (2015) Spatial and temporal responses in stomatal behaviour, photosynthesis and implications for water-use efficiency. In: Mancuso S, Shabala S (eds) *Rhythms in plants*. Springer, Cham, pp 97–119.
- Kromdijk J, Glowacka K, Leonelli L, Gabilly ST, Iwai M, Niyogi KK, Long SP. Improving photosynthesis and crop productivity by accelerating recovery from photoprotection. *Science.* 2016;354(6314):857–61.
- Badger MR, Fallahi H, Kaines S, Takahashi S. Chlorophyll fluorescence screening of *Arabidopsis thaliana* for CO<sub>2</sub> sensitive photorespiration and photoinhibition mutants. *Funct Plant Biol.* 2009;36:867–73.
- Eisenhut M, Weber AP. Improving crop yield. *Science.* 2019;363(6422):32–3.
- Tottman D. The decimal code for the growth stages of cereals, with illustrations. *Ann Appl Biol.* 1987;110(2):441–54.
- Schreiber U, Schliwa U, Bilger W. Continuous recording of photochemical and non-photochemical chlorophyll fluorescence quenching with a new type of modulation fluorometer. *Photosynth Res.* 1986;10(1–2):51–62.
- Baker NR, Rosenqvist E. Applications of chlorophyll fluorescence can improve crop production strategies: an examination of future possibilities. *J Exp Bot.* 2004;55(403):1607–21.
- Sayed O. Chlorophyll fluorescence as a tool in cereal crop research. *Photosynthetica.* 2003;41(3):321–30.
- Baker NR, Oxborough K. Chlorophyll fluorescence as a probe of photosynthetic productivity, vol. 19. Berlin: Springer; 2004.
- Hubbart S, Ajigboye OO, Horton P, Murchie EH. The photoprotective protein PsbS exerts control over CO<sub>2</sub> assimilation rate in fluctuating light in rice. *Plant J.* 2012;71(3):402–12.
- Glowacka K, Kromdijk J, Kucera K, Xie J, Cavanagh AP, Leonelli L, Leakey AD, Ort DR, Niyogi KK, Long SP. Photosystem II subunit S overexpression

- increases the efficiency of water use in a field-grown crop. *Nat Commun.* 2018;9(1):868.
43. Bertoni G. Pentapeptide protection of botrytis-infected tomato plants by phytosulfokine. In: *Am Soc Plant Biol*; 2018.
  44. Lidon F, Loureiro A, Vieira D, Bilho E, Nobre P, Costa R. Photoinhibition in chilling stressed wheat and maize. *Photosynthetica.* 2001;39(2):161–6.
  45. Hayden DB, Baker NR, Percival MP, Beckwith PB. Modification of the photosystem II light-harvesting chlorophyll ab protein complex in maize during chill-induced photoinhibition. *Biochim Biophys Acta Bioenergetics.* 1986;851(1):86–92.
  46. Savitch LV, Gray GR, Huner NP. Feedback-limited photosynthesis and regulation of sucrose-starch accumulation during cold acclimation and low-temperature stress in a spring and winter wheat. *Planta.* 1997;201(1):18–26.
  47. Johnson DA, Richards RA, Turner NC. Yield, water relations, gas exchange, and surface reflectances of near-isogenic wheat lines differing in glaucousness 1. *Crop Sci.* 1983;23(2):318–25.
  48. Shepherd T, Griffiths DW. The effects of stress on plant cuticular waxes. *New Phytol.* 2006;171(3):469–99.
  49. Violet-Chabrand SR, Matthews JS, McAusland L, Blatt MR, Griffiths H, Lawson T. Temporal dynamics of stomatal behavior: modeling and implications for photosynthesis and water use. *Plant Physiol.* 2017;174(2):603–13.
  50. Lawson T, Kramer DM, Raines CA. Improving yield by exploiting mechanisms underlying natural variation of photosynthesis. *Curr Opin Biotechnol.* 2012;23(2):215–20.
  51. Reynolds M, Foulkes J, Furbank R, Griffiths S, King J, Murchie E, Parry M, Slafer G. Achieving yield gains in wheat. *Plant, Cell Environ.* 2012;35(10):1799–823.
  52. Murchie E, Horton P. Acclimation of photosynthesis to irradiance and spectral quality in British plant species: chlorophyll content, photosynthetic capacity and habitat preference. *Plant Cell Environ.* 1997;20(4):438–48.
  53. Murchie EH, Niyogi KK. Manipulation of photoprotection to improve plant photosynthesis. *Plant Physiol.* 2011;155(1):86–114.
  54. Verhoeven AS, Demmig-Adams B, Adams WW III. Enhanced employment of the xanthophyll cycle and thermal energy dissipation in spinach exposed to high light and N stress. *Plant Physiol.* 1997;113(3):817–24.
  55. Demmig-Adams B, Adams W. Photoprotection and other responses of plants to high light stress. *Annu Rev Plant Biol.* 1992;43(1):599–626.
  56. Li X-P, BjoErkman O, Shih C, Grossman AR, Rosenquist M, Jansson S, Niyogi KK. A pigment-binding protein essential for regulation of photosynthetic light harvesting. *Nature.* 2000;403(6768):391.
  57. King J, Grewal S, Yang CY, Hubbart S, Scholefield D, Ashling S, Edwards KJ, Allen AM, Burridge A, Bloor C. A step change in the transfer of interspecific variation into wheat from *Amblyopyrum muticum*. *Plant Biotechnol J.* 2017;15(2):217–26.
  58. Zamir D. Improving plant breeding with exotic genetic libraries. *Nat Rev Genet.* 2001;2(12):983.

### Publisher's Note

Springer Nature remains neutral with regard to jurisdictional claims in published maps and institutional affiliations.

Ready to submit your research? Choose BMC and benefit from:

- fast, convenient online submission
- thorough peer review by experienced researchers in your field
- rapid publication on acceptance
- support for research data, including large and complex data types
- gold Open Access which fosters wider collaboration and increased citations
- maximum visibility for your research: over 100M website views per year

At BMC, research is always in progress.

Learn more [biomedcentral.com/submissions](https://biomedcentral.com/submissions)

